Cement & Concrete Composites 34 (2012) 1061–1066

Contents lists available at SciVerse ScienceDirect

Cement & Concrete Composites

journal homepage: www.elsevier.com/locate/cemconcomp

Strength and ductility of RC beams strengthened with steel-reinforced strain hardening cementitious composites

Mohamed Hussein [a,b,*], Minoru Kunieda [a], Hikaru Nakamura [a]

[a] Department of Civil Engineering, Nagoya University, Chikusa-ku, Nagoya 464-8603, Japan
[b] Department of Structural Engineering, Tanta University, Tanta 31511, Egypt

ARTICLE INFO

Article history:
Received 5 April 2010
Received in revised form 16 May 2012
Accepted 9 June 2012
Available online 16 June 2012

Keywords:
Concrete beams
SHCC
Localized fracture
Reinforcement
Enhancement
Ductility

ABSTRACT

Strengthening of Reinforced Concrete (RC) beams using strain hardening cementitious composites (SHCCs) layer cast to their soffit has recently been investigated. That work confirmed that strain localization occurs in the SHCC-strengthening layer, which severely limits the ductility of the strengthened beam. This paper reports the ductility enhancement achieved in tests on reinforced concrete beams that were strengthened with lightly steel-reinforced SHCC layer (0.3% and 0.6% steel reinforcement ratio). It has been found that the combination of the SHCC and a small amount of steel reinforcement helps develop higher strain in the SHCC strengthening layer at ultimate load and eliminates the observed early strain localization. The recorded averaged strain at ultimate load of SHCC-strengthening layer provided with 0.3% and 0.6% steel reinforcement was 2.10 and 3.76 times that of an unreinforced SHCC layer. Also, use of a 0.6% reinforcement ratio changed the mode of failure of the SHCC-strengthened beams from brittle to more ductile. Moreover, the SHCC-strengthening layer with 0.6% reinforcement ratio was able to develop uniformly distributed visible cracks, which were the only indication that failure was imminent. It needs to be emphasized that strengthening of RC structures using an unreinforced SHCC layer may lead to a brittle failure.

1. Introduction

Because of increasing service loads and more stringent code stipulations, many structures are becoming functionally obsolete because the original designs no longer meet current standards and consequently a significant number of our RC elements are in urgent need of strengthening or rehabilitation. One of the most important factors affecting the successful strengthening of structures is the selection of strengthening material. Compatibility between substrate and strengthening material is a key factor in selection of strengthening material. Cement-based materials are generally suitable for repairing and strengthening of concrete structures due to their compatible mechanical and physical properties, as well as other important considerations such as cost, availability, and constructability [1]. In the past decade, fiber reinforced cementitious composites with higher ductility such as strain hardening cementitious composites (SHCCs) have been developed. This progress has been due to the developments in fiber, matrix, and process technology, as well as better understanding of the fundamental micromechanics governing composite behavior [2]. SHCC promises to be used in a wide variety of civil engineering applications, as summarized in Japan Concrete Institute (JCI 2002) [3] and by Kunieda and Rokugo [4].

One of the most promising areas of application of this material is in the repair of concrete structures. Several investigations on the advantages of structures repaired by SHCC have been carried out. Lim and Li [5] demonstrated the advantages of an interface crack trapping mechanism within SHCC/RC composites. The effects of surface preparation on the fracture behavior of SHCC/RC composites were discussed by Kamada and Li [6]. Also, Li [7] addressed the required properties for repair materials to obtain durable repaired concrete structures. Numerous studies have shown that concrete rehabilitation using strain hardening cementitious composites (SHCC) is very successful at restoring or increasing the strength of concrete members [8–15]. Martinola et al. [16] investigated the structural behavior of strengthened and repaired beams by using a thin layer of high performance fiber reinforced concrete. Their test results showed that the effectiveness of the proposed technique in improving the bearing capacity, in both the cases of strengthening and repair. Kamal [17] investigated the structural performance of simply supported reinforced concrete beams strengthened with Ultra High Performance Strain Hardening Cementitious Composite (UHP-SHCC) layer cast to their soffit. This material was developed and tested by Kunieda et al. [18] and it combines excellent protective performance, similar to that of ultra high performance fiber reinforced concrete (UHPFRC), with a

* Corresponding author at: Department of Structural Engineering, Tanta University, Tanta 31511, Egypt. Tel.: +20 122 373 7849.
E-mail address: m_hussein_20@yahoo.com (M. Hussein).

0958-9465/$ - see front matter © 2012 Elsevier Ltd. All rights reserved.
http://dx.doi.org/10.1016/j.cemconcomp.2012.06.004

significantly higher tensile strain hardening (up to 2%) at peak strength. His test results showed that failure of the strengthened beams was due to sudden rupture of the UHP-SHCC strengthening layer at a significantly less final deflection compared with unstrengthened beams. Also, the strengthened beams were unable to sustain inelastic deformation prior to collapse. Strain localization occurred prematurely in the strengthening layer, which severely limits the ductility of the strengthened beam.

The present work examines the effectiveness of providing the UHP-SHCC strengthening layer with a small amount of steel reinforcement. The role of the steel reinforcement is to counteract the stiffness degradation of UHP-SHCC strengthening layer, caused by cracking, and consequently eliminates the observed early strain localization. This paper presents the results of experimental tests on: two RC control beams, four RC beams strengthened with a steel-reinforced UHP-SHCC layer, two RC beams strengthened with an unreinforced UHP-SHCC layer, and four RC beams strengthened with a steel-reinforced mortar layer. All strengthening layers had a thickness of 50 mm. Deformation behavior, cracking development and strain distribution along the beams' axis are investigated. Effect of varying the steel amount on crack distribution and mode of failure is presented.

2. Experimental program

2.1. Material properties

The mix proportions of the UHP-SHCC used as a strengthening material in this study are listed in Table 1 [1]. Water to binder ratio (W/B) was 0.20. Low heat Portland cement (density: 3.14 g/cm^3) was used, and 15% of the design cement content was replaced by silica fume. Quartz sand with diameter less than 0.5 mm was used as a fine aggregate. High strength polyethylene (PE) fiber was chosen for UHP-SHCC and its volume in mix was 1.5%. The diameter and length of the PE fibers were 0.012 mm and 6 mm, respectively. The tensile behavior of the used UHP-SHCC was characterized by testing of ten dumbbell-shaped specimen (tested cross-section: 10 × 30 mm) in uniaxial tensile test. The averaged tensile strength and ultimate tensile strain (strain at ultimate load) of the used UHP-SHCC at the age of 28 days were determined to be 8 MPa and 1.5% respectively. Fig. 1 shows a sample of the stress–strain relationship measured from the uniaxial tensile tests. To characterize the compressive properties of the used UHP-SHCC, 6 cylindrical specimens having a size of 50 × 100 mm were tested at the age of 28 days and the averaged compressive strength was determined to be 111 MPa.

The used concrete was made from a mix of ordinary Portland cement, natural sand, and gravel with the mixture proportions shown in Table 1. The averaged compressive strength of the used substrate concrete was determined to be 25 MPa based on the compressive test results of six cylindrical specimens (ϕ 100 × 200 mm). The mix proportions of the used mortar, shown in Table 1, were selected to achieve a compressive strength of 25 MPa, the same as the substrate concrete strength. The averaged compressive strength of the used mortar was determined to be 26 MPa based on the compressive test results of six cylindrical specimens (ϕ 100 × 200 mm). In order to determine the mechanical properties of the used 6 mm diameter (D6) rebar, tensile tests were performed on three specimens. The mean value of tensile yield strength, ultimate strength and Young's modulus were 437 MPa, 631 MPa and 190 GPa respectively. For the used 10 mm diameter (D10) rebar, the mean value of tensile yield strength, ultimate strength and Young's modulus were 360 MPa, 631 MPa and 200 GPa respectively.

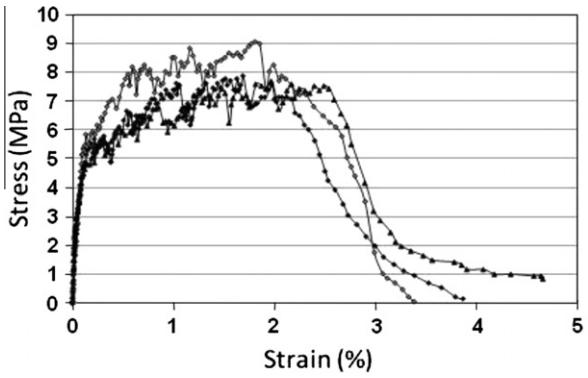

Fig. 1. Stress–strain relationship for uniaxial tensile tests of UHP-SHCC materials.

2.2. Test specimens

Four-point bending flexural tests were conducted up to failure on two RC control beams, six RC beams strengthened with 50 mm steel reinforced UHP-SHCC layer thickness, and four RC beams strengthened with 50 mm reinforced mortar layer thickness. Both UHP-SHCC and reinforced mortar layers were cast at the beams' tension side. All the beams had nominal dimensions of 200 mm width × 200 mm height × 1800 mm length. Two 10 mm diameter (D10) rebars were used as tension reinforcement for all the beams. Stirrups of 6 mm diameter (D6) were used in the shear span at the interval of 90 mm, as shown in Fig. 2. Also, D6 rebars were used as UHP-SHCC reinforcement with two reinforcement ratios as shown in Table 2. The beams were demoulded at the age of 2 days, and their bottom surface (tension reinforcement side) was washed out using a retarder to obtain a rough surface. Following the wash-out process the specimens were covered with wet towels for additional 26 days. At the age of 28 days, UHP-SHCC strengthening layer was cast with 50 mm thickness in the beams' tension side (rebar side). For the UHP-SHCC-strengthened beams, two beams were strengthened using unreinforced UHP-SHCC layer, whereas four beams were strengthened with steel reinforced UHP-SHCC layer with variable reinforcement ratio according to Table 2. The contribution from the steel bars, reinforcing the UHP-SHCC layer, to the beam's load-carrying capacity was evaluated by testing of four RC beams strengthened with 50 mm thickness steel

Table 1
Mix proportions of UHP-SHCC, substrate concrete, and reinforced mortar layer.

Material	Water/binder[a]	Unit content (kg/m^3)							
		Water content	Cement	Silica fume	Sand	Coarse aggregate	Super plasticizer	Air reducer	PE fiber (6 mm)
UHP-SHCC	0.20	292	1243	223	149	–	14.9	2.98	14.6
Substrate concrete	0.63	185	294	–	843	919	–	–	–
Reinforced mortar	0.50	147	294	–	1762	–	–	–	–

[a] Binder = cement + silica fume.

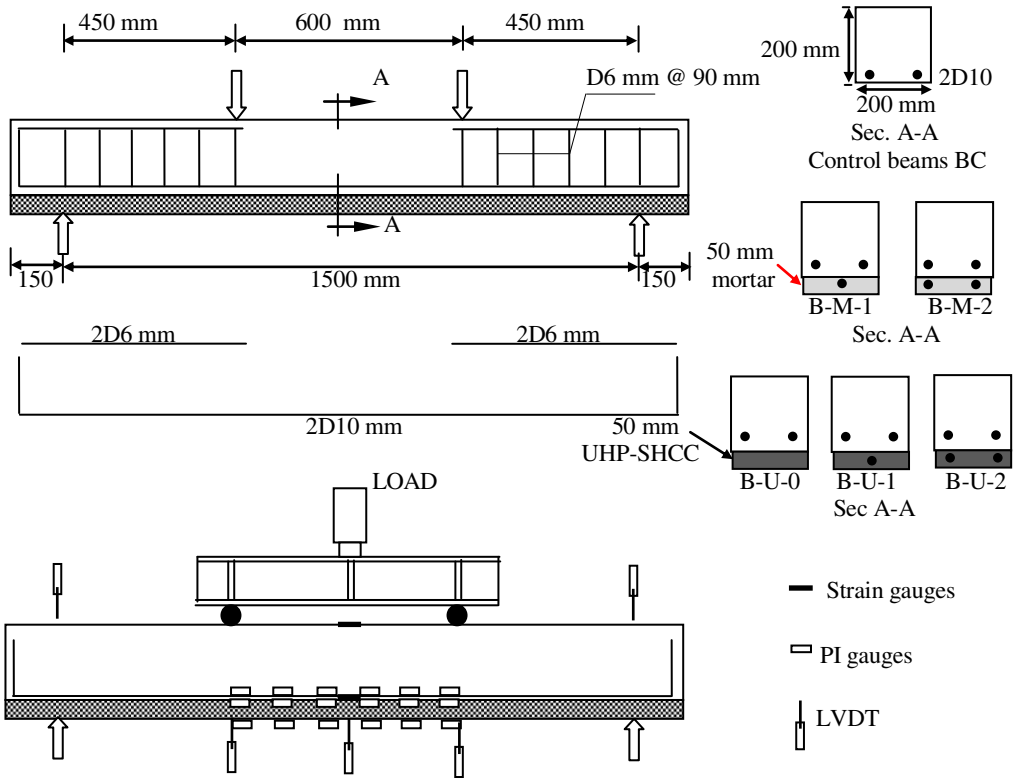

Fig. 2. Test setup and specimens' details.

Table 2
Description of test beams.

Specimen	Dimensions (mm)	Strengthening layer thickness (mm)	Strengthening layer reinforcement			No. of tested beams
			UHP-SHCC	Reinforced mortar	Reinforcement ratio%	
BC	200 × 200 × 1800	–	–	–	–	2
B-U-0	200 × 200 × 1800	50 (UHP-SHCC)	–	–	0.0	2
B-U-1	200 × 200 × 1800	50 (UHP-SHCC)	1 D6	–	0.3	2
B-U-2	200 × 200 × 1800	50 (UHP-SHCC)	2 D6		0.6	2
B-M-1	200 × 200 × 1800	50 Reinforced mortar		1 D6	0.3	2
B-M-2	200 × 200 × 1800	50 Reinforced mortar		2 D6	0.6	2

reinforced mortar layer. The mortar layer was reinforced with the same UHP-SHCC layer reinforcement ratio as shown in Table 2.

2.3. Test setup and procedure

All the beams were loaded in four-point bending. The load was applied using a hydraulic actuator through a spreader steel beam to the specimen. Each specimen spanned 1,500 mm and was loaded symmetrically about its centerline at two points 600 mm apart. A load cell was attached to the loading actuator to record the applied load. One strain gauge was bonded to the top concrete surface of each specimen at midspan, to record the compression strain in the extreme concrete fibers. One strain gauge was bonded to each rebar at its midspan. During the test, UHP-SHCC strengthening layer's strains were recorded by six Pi-shaped displacement transducers with a gauge length of 100 mm applied on layer's bottom side as shown in Fig. 2, whereas six additional Pi-shaped displacement transducers were used to record the substrate concrete strains at concrete-UHP-SHCC layer interface as shown in Fig. 2. Displacements at loading points, midspan and supports were measured by LVDT (stroke = 50 mm, sensitivity = 0.005 mm). An automatic data acquisition system was used to monitor loading, displacements and strains. The instrumentation used to monitor the behavior of the beams during testing is shown in Fig. 2.

3. Test results and discussion

3.1. Loads and failure modes

The unstrengthened control beams failed, as expected, in flexure with extensive yielding of the tension steel, followed by crushing of the concrete in the compression zone. Failure of all the UHP-SHCC strengthened beams was by rupture of the strengthening layer, which occurred near the midspan or loading points, after yielding of the reinforcing steel bars and before concrete crushing, according to strain monitoring realized during the test. Formation of visible cracks in the UHP-SHCC strengthening layer closer to the central span was the only indication that failure was imminent. No signals of degradation, before failure, could be seen at the bottom side of the UHP-SHCC strengthening layer. It was possible to verify on the experimental results that the development of a crack in the concrete substrate might produce high strain concentration points

Table 3
Cracking, yield, and ultimate load and displacement values.

Beam	Cracking				Yield		Ultimate load	
	Substrate conc.		UHP-SHCC		Main reinforcement			
	Load (kN)	Disp. (mm)	Load (kN)	Disp. (mm)	Load (kN)	Disp. (mm)	Load (kN)	Disp. (mm)
BC	19.0	1.09	–	–	41.0	3.50	49.0	40.15
B-U-0	35.0	0.52	50.0	0.95	78.3	3.92	82.3	4.77
B-U-1	35.8	0.48	50.5	1.02	82.2	4.00	88.9	5.96
B-U-2	35.9	0.54	51.0	1.04	95.5	4.69	100.7	11.00
B-M-1	31.0	0.46	–	–	51.0	3.60	62.0	32.05
B-M-2	31.5	0.47	–	–	60.0	3.50	74.4	37.05

in the UHP-SHCC strengthening layer, inducing the tensile failure of the strengthening layer. Although failure of the beams strengthened using steel reinforced and unreinforced UHP-SHCC layer was by rupture of UHP-SHCC layer, formation of distributed visible cracks in UHP-SHCC layer for beam B-U-2 made its failure more predictable than other beams. When 0.6% reinforcement ratio was used (B-U-2) there seems to be a delay in the formation of wide cracks in the UHP-SHCC layer, which allows the beam to achieve considerably higher deflection and ultimate loads compared to beam B-U-0. On the other hand, the reinforced mortar strengthened beams failed, as expected, in flexure with extensive yielding of the tension steel, followed by crushing of the concrete in the compression zone.

The ultimate loads, the cracking loads, and the yielding loads are shown in Table 3. Experimental results reported in Table 3 indicate an increase of varying degrees in the cracking load for all of the strengthened beams over that of the control beam BC. This is to be expected, partially because of the stiffening of the beams due to the application of the strengthening layer. The greatest increase in cracking load was obtained in beam B-U-2, which resulted in a 88.9% increase over the control beam, followed by beams B-U-1 and B-U-0, exhibiting increases in the cracking load of 88.4% and 84.2%, respectively. Beams B-M-1 and B-M-2 exhibited similar increases in the cracking load of 63% and 66%, respectively. The UHP-SHCC applied to beams B-U-0, B-U-1, and B-U-2 had a greater axial and flexural stiffness, as described above, in comparison to the other application (reinforced mortar), which may make some contribution to the greater increase in the cracking load.

As shown in Table 3 the greatest increase in the yield load over the control beam was obtained by beam B-U-2 at 133%. Beams B-U-0 and B-U-1 obtained comparable increase in the yield load of 91% and 100%, respectively. Beams B-M-1 and B-M-2, exhibited increases in the yielding load of 24 and 46%, respectively.

Ultimate loads registered for all tested beams are shown in Table 3. The results show that the ultimate load increased about 68%, 81% and 106% in beams B-U-0, B-U-1 and B-U-2, over the control beam BC, respectively, whereas the ultimate load capacity was increased by 27% and 52%, for beams B-M-1 and B-M-2, respectively.

3.2. Load versus deflection response at midspan

Fig. 3 shows the measured load–deflection response for the beams tested. The control beam BC showed the usual elastic and inelastic parts of its deflection behavior and failed, as expected, due to yielding of the tensile steel reinforcement prior to crushing of the concrete at significantly high final deflections than the UHP-SHCC strengthened beams. The characteristics of the load–deflection behavior of beam B-U-0 may be summarized as follows. Initially, the behavior is linear, with cracks appearing near the beam's midspan the curve begins to deviate from the linear path. After the strengthened beam reaches its ultimate load, the load

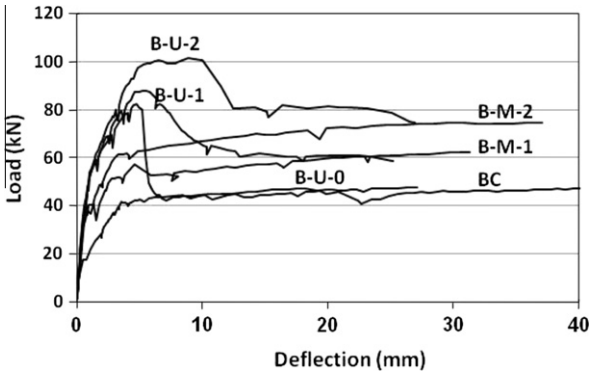

Fig. 3. Load–midspan deflection curve.

drops rapidly from the peak to a significantly lower load level round the control beam (BC) capacity, and then the beam's behavior was controlled by the original steel reinforcement as before the application of the strengthening scheme. Beams B-U-1 and B-U-2, provided with 0.3% and 0.6% reinforcement ratio respectively, both demonstrated the same load–deflection response, as beam B-U-0, up to ultimate load. However, after the beams reached their ultimate load, as can be seen in Fig. 3, they were able to sustain inelastic deformation prior to collapse, without significant loss in resistance. Also, the sustained inelastic deformation was increased by increasing reinforcement ratio. After the strengthened beams reached their ultimate load, and contrary to the observed behavior of beam B-U-0, the curve demonstrated a softening tail (tension-softening curve), and the load drops gradually from the peak to a load level round the reinforced mortar strengthened beams' load carrying capacity. Thereafter, the beams' behavior was controlled by the steel reinforcement, and it was very similar to the recorded post-yielding behavior of the reinforced mortar beams as shown in Fig. 3.

3.3. Crack behavior

Table 4 shows the results of crack width visual inspection, taken when the beams were subjected to moderate (32 kN) and high (48 kN) loads, as well as after being subjected to the ultimate load achieved. It can be seen that cracks were much wider on the control beam, for all loads. The first crack was noticed on the control beam when the applied load reached about 19 kN and, at the ultimate load (49 kN), the maximum crack width on the constant moment region was 3.5 mm. Crack width of the UHP-SHCC strengthened beams B-U-0, B-U-1, and B-U-2, at about 48 kN, where 0.04 mm, seventy times lower than in the control beam. Also, their crack widths at ultimate load still lower, reaching 0.2 mm (B-U-0 and B-U-1) and 0.25 mm (B-U-2).

The examination of the UHP-SHCC strengthened beams immediately before failure showed that the number of developed cracks

Table 4
Maximum crack width at 32 kN, 48 kN and at ultimate load.

Beam	Maximum crack width developed in the substrate concrete		
	At 32 kN (mm)	At 48 kN (mm)	At ultimate load (mm)
BC	0.25	3.50	3.50
B-U-0	–	0.05	0.20
B-U-1	–	0.05	0.20
B-U-2	–	0.05	0.25
B-M-1	0.05	0.30	3.00
B-M-2	0.05	0.25	3.50

in the substrate concrete was not reduced when compared to the number of cracks of the control beam at failure. However, the maximum crack width was much lower, even when ultimate loads achieved were much higher.

The UHP-SHCC crack patterns of reference and reinforced layers, shown in Fig. 4, clearly reveals the significant improvement in the UHP-SHCC cracking behavior provided with the proposed steel reinforcement. It can be clearly seen from the summary of the test results presented in Table 5, that while increasing the reinforcement ratio the averaged crack spacing will gradually be reduced whereas the number of developed cracks will be increased. Compared to the number of cracks developed in unreinforced UHP-SHCC layer for beam B-U-0, 0.6% reinforcement ratio enabled beam B-U-2 to develop 120 cracks, more than twice the number in beam B-U-0.

3.4. Averaged strain in UHP-SHCC strengthening layer at ultimate load

The averaged tensile strain experienced by the UHP-SHCC strengthening layers at failure load for each beam, is shown in Table 6. These strains were obtained by dividing the total elongation of the UHP-SHCC layer, in the constant moment region, with their length. For beam B-U-0, the experimental results show that without reinforcement the UHP-SHCC layers ruptured at about 17% of their ultimate strain capacity obtained from the dumbbell-shaped specimens' tensile test. Providing the strengthening layer with 0.3% steel reinforcement ratio increased its averaged tension strain at failure to 35% of its strain capacity. Increasing reinforcement ratio to 0.6% enabled the UHP-SHCC strengthening layer to attain an averaged strain at ultimate load of 0.924%, which represents about 62% of its strain capacity.

The mean strain versus load of the test beams is illustrated in Fig. 5. For all the beams, load versus mean strain relationship is linear before cracking. After the strengthened beam reached its ultimate load, the unreinforced UHP-SHCC layer ruptured suddenly at a significantly less average strain compared to the steel reinforced UHP-SHCC layers. As shown in Fig. 5, the effect of the steel reinforcement was to enable beams B-U-1 and B-U-2 to attain high averaged strain at failure compared to beam B-U-0.

3.5. Ductility analysis

In strengthening of RC structures with UHP-SHCC it is notable that the increase in strength and stiffness is sometimes attained at the expense of a loss in ductility, or loss of capacity of the structures to deflect inelastically while sustaining a significant percentage of its maximum load. Ductility is an important property for safe design of strengthening of any structural element. As UHP-SHCC strengthening is a relative recent strengthening strategy, understanding the effect of this technique on the ductility of a RC member is crucial. In the present work, the ductility indexes are expressed as the ratio between the deflection, or curvature, at an ultimate condition (Δ_u and ϕ_u, respectively), and the deflection, or curvature, at the yield load (Δ_y and ϕ_y, respectively), as follows:

$$\mu_{\Delta} = \Delta_u/\Delta_y \tag{1}$$

and

$$\mu_{\phi} = \phi_u/\phi_y \tag{2}$$

Table 7 lists the values of the ductility indices for all tested beams. According to the FIB (1990) [19] recommendations, the minimum ductility index, in terms of curvature, should be approximately 1.7 and 2.6 for concrete types C35/45 or lower and concrete types higher than C35/45, respectively. The ductility index should exceed this minimum value to prevent the occurrence of sudden failure in the strengthened flexural members. The minimum acceptable ductility index ensures that the internal reinforcement experiences plastic deformation in order to provide the desired warning prior to failure of the member. The proposed steel reinforcement enhanced the post cracking behavior of UHP-SHCC provides a much more ductile behavior for the steel reinforced UHP-SHCC strengthening technique compared to the unreinforced UHP-SHCC strengthening technique. As shown in Table 7, the curvature ductility indexes (μ_{ϕ}) of all the UHP-SHCC-strengthened beams are lower than the value obtained for the control beam (18.63). However, the curvature ductility index (μ_{ϕ}) of beams B-U-1 (1.62),

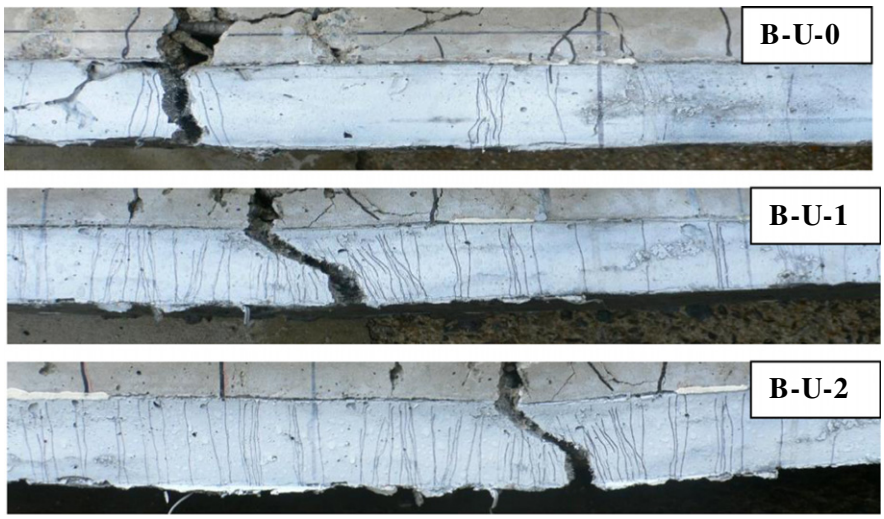

Fig. 4. Final cracking patterns for UHP-SHCC strengthening layer.

Table 5
Experimental data for cracking characteristics of UHP-SHCC layer at ultimate load.

Beam	Cracks developed in the UHP-SHCC layer		
	S_{av} (mm)	S_{max} (mm)	N
B-U-0	20.0	100	50
B-U-1	7.5	30	100
B-U-2	5.3	30	120

S_{av} = average crack spacing, S_{max} = maximum crack spacing, and N = number of cracks.

Table 6
UHP-SHCC ultimate strain values.

Beam	UHP-SHCC			
	$\varepsilon_{u\text{-}min}$ (%)	$\varepsilon_{u\text{-}max}$ (%)	$\varepsilon_{u\text{-}av}$ (%)	$(\varepsilon_{u\text{-}av}/\varepsilon_{u\text{-}av\ (B\text{-}U\text{-}0)}$
B-U-0	0.106	0.610	0.252	1.00
B-U-1	0.200	1.001	0.520	2.06
B-U-2	0.440	1.860	0.924	3.67

$\varepsilon_{u\text{-}min}$, $\varepsilon_{u\text{-}max}$, and $\varepsilon_{u\text{-}av}$ = minimum and average UHP-SHCC strain at ultimate load.

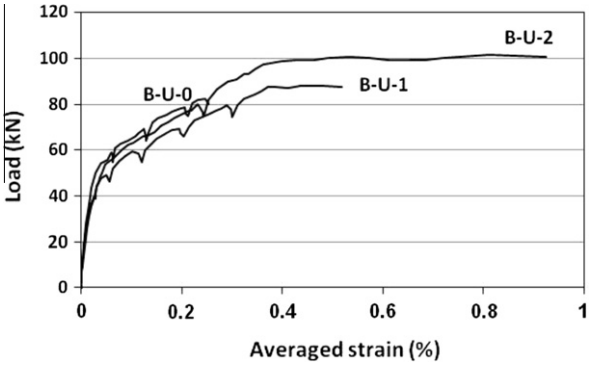

Fig. 5. Load versus average strain of the UHP-SHCC layers.

Table 7
Ductility ratios of tested beams.

Beams	Δ_y (mm)	Δ_u (mm)	Ductility index (μ_Δ)	Yield curvature (km^{-1})	Ultimate curvature (km^{-1})	Ductility index (μ_ϕ)
BC	3.5	40.15	11.47	10.22	190.40	18.63
B-U-0	3.92	4.77	1.22	10.44	12.78	1.22
B-U-1	4.00	5.96	1.49	10.89	17.56	1.62
B-U-2	4.69	11.00	2.35	11.10	44.40	4.00
B-M-1	3.60	32.05	8.90	10.11	136.83	13.53
B-M-2	3.50	37.05	10.59	11.44	128.95	11.27

and B-U-2 (4.00), strengthened with steel reinforced UHP-SHCC layer, are higher than the one obtained for beam B-U-0 (1.22), strengthened with unreinforced UHP-SHCC layer. The results seem to indicate that the use of steel reinforcement can successfully enhance the ductility of UHP-SHCC strengthened beams. Moreover, 0.6% steel reinforcement enabled beam B-U-2 to attain a curvature ductility index (μ_ϕ) of 4, which, according to FIB (1990) [19] recommendations, is adequate to guarantee satisfactory ductility.

4. Conclusions

This study has compared the flexural behavior of reinforced concrete beams strengthened with steel reinforced and unreinforced strain hardening cementitious composites layer cast to their soffit. The main conclusions drawn from the study are as follows:

1. It was confirmed that the development of a crack in the concrete substrate might produce high strain concentration points in the UHP-SHCC strengthening layer, and induce localized failure of the strengthening layer. However, when the proposed steel reinforcement is used, crack localization in the UHP-SHCC strengthening layer is delayed. This might be attributed to a greater resistance to local failure of steel-reinforced UHP-SHCC.
2. The combination of the proposed steel reinforcement (reinforcement ratio = 0.6%) and UHP-SHCC, used to strengthen beam B-U-2, was able to increase its load-carrying capacity to 100 kN, which is twice that of the control beam B-C. Moreover, it fulfilled the ductility criterion recommended by CEB-FIB (1990) [19] .
3. The load–deflection response of the strengthened beams indicates that the use of small amount of steel reinforcement within the UHP-SHCC strengthening layer significantly enhanced their post peak behavior. Consequently, the role of the small amount of steel reinforcement is to reduce the stiffness degradation of the UHP-SHCC strengthening layer caused by cracking.

References

[1] Kamal A, Kunieda M, Ueda N, Nakamura H. Evaluation of crack opening performance of a repair material with strain hardening behavior. J Cem Concr Compos 2008;30(10):863–71.
[2] Li VC, Horikoshi T, Ogawa A, Torigoe S, Saito T. Micromechanics-based durability study of polyvinyl alcohol-engineered cementitious composite (PVA-ECC). ACI Mater J 2004;101(1):242–8.
[3] Proceedings of the JCI international workshop on ductile fiber reinforced cementitious composites (DFRCC), Japan Concrete Institute, October 2002.
[4] Kunieda M, Rokugo K. Recent progress of SHCC in Japan-required performance and applications. J Adv Concr Technol 2006;4(1):19–33.
[5] Lim YM, Li VC. Durable repair of aged infrastructures using trapping mechanism of engineered cementitious composites. J Cem Concr Compos 1997;19(4):171–85.
[6] Kamada T, Li VC. The effects of surface preparation on the fracture behavior of ECC/concrete repair system. J Cem Concr Compos 2000;22(6):423–31.
[7] Li VC. High performance fiber reinforced cementitious composites as durable material for concrete structure repair. Int J Restor Build Monument 2004;10(2):163–80.
[8] Horii H, Matsuoka S, Kabele P, Takeuchi S, Li VC, Kanda T. On the prediction method for the structural performance of repaired/retrofitted structures. In: Proceedings FRAMCOS-3. Fracture mechanics of concrete structures. Freiburg (Germany): AEDIFICATIO Publishers; 1998. p. 1739–50.
[9] Kamal A, Kunieda M, Ueda N, Nakamura H. Assessment of strengthening effect on RC beams with UHP-SHCC. In: Proceeding of JCI annual meeting, CD: file No. 3248, 2008. p. 1483–88.
[10] Maalej M, Li VC. Introduction of strain hardening engineered cementitious composites in the design of reinforced concrete flexural members for improved durability. J Am Concr Ins Struct 1995;92(2):167–76.
[11] Li VC. From micromechanics to structural engineering – the design of cementitious composites for civil engineering applications. JSCE J Struct Mech Earthquakes Eng 1993;10(2).
[12] Li VC. ECC for repair and retrofit in concrete structures. In: Fracture mechanics of concrete structures. Proceedings FRAMCOS-3. Freiburg (Germany): AEDIFICATIO Publishers; 1998. p. 1715–26.
[13] Li VC, Horii H, Kabele P, Kanda T, Lim YM. Repair and retrofit with engineered cementitious composites. Int J Eng Fract Mech 2000;65(2–3):317–34.
[14] Shin SK, Kim JJH, Lim YM. Investigation of the strengthening effect of DFRCC applied to plain concrete beams. J Cem Concr Compos 2007;29(6):465–73.
[15] Matsumoto T, Mihashi H. JCI-DFRCC Summary report on DFRCC terminologies and application concepts. In: Proceedings of the JCI international workshop on ductile fiber reinforced cementitious composites; 2002. p. 59–66.
[16] Martinola G, Meda A, Plizzari GA, Rinaldi Z. Strengthening and repair of RC beams with fiber reinforced concrete. J Cem Concr Compos 2010;32(9):731–9.
[17] Kamal A. Material development of UHP-SHCC for repair applications and its evaluation. Ph.D. thesis. Nagoya University; 2008.
[18] Kunieda M, Denarié E, Brühwiler E, Nakamura H. Challenges for strain hardening cementitious composites – deformability versus matrix density. In: Proceedings of the fifth international RILEM workshop on HPFRCC; 2007. p. 31–8.
[19] Comite Euro-International du Beton-Federation International de la Precon Straente (CEB-FIP). Model code, Thomas Telford, London; 1990.